Characterization of metal free D- (π-A)$_2$ organic dye and its application as co-sensitizer along with N719 dye for efficient dye sensitized solar cells

M Singh[1], R Kurchania[1*], A Pockett[2], R J Ball[3], E N Koukaras[4], P J Cameron[2], G D Sharma[5*]

[1]*Department of Physics, Maulana Azad National Institute of Technology (MANIT), Bhopal 462051, Madhya Pradesh, India*
[2]*Department of Chemistry, University of Bath, Bath, BA2 7AY, United Kingdom*
[3]*Department of Architecture and Civil Engineering, University of Bath, Bath, BA2 7AY, United Kingdom*
[4]*Institute of Chemical Engineering Science, Foundation for Research & Technology Hellas, Stadiou Str. Platani, Patras, 26504 Greece*
[5]*R & D Center for Engineering and Science, JEC Group of colleges JEC Campus, Kukas, Jaipur 303101, Rajasthan, India*

Abstract

The optical, electrochemical and density functional theory molecular simulation of a metal free D-(π-A)$_2$ i.e. 3,3'-(5,5'-(9-hexyl-9H-carbazole-3,6-diyl)bis(thiophene-5,2-diyl))bis(2-cyanoacrylic acid denoted as **D**) has been investigated**.** A step wise cosensitization of **D** with N719 dye is adopted to enhance the power conversion efficiency of dye sensitized solar cells. The metal free dye possesses strong absorption in the 370-450 nm wavelength range and effectively overcome the competitive light absorption by I_3^- / I^-. The N719/**D** cosensitized dye sensitized solar cell shows a power conversion efficiency of about 7.24 % which is higher than the dye sensitized solar cells based on either N719 (5.78 %) or **D** (3.95 %) sensitizers. The improved power conversion efficiency of the cosensitized dye sensitized solar cell is attributed to the combined enhancement of both short circuit photocurrent and open circuit voltage. The short circuit photocurrent improvement is attributed to the increase in the both light harvesting efficiency of the cosensitized photoanode and charge collection efficiency of the dye sensitized solar cell. However, the open circuit voltage is improved due to better adsorption and surface coverage of TiO_2 on cosensitization and an associated reduction in the back electron recombination with increased electron lifetime. These effects are analyzed using electrochemical impedance spectroscopy and dark current–voltage measurements of the dye sensitized solar cells.

Key words: Co-sensitization, metal free D-(π-A)$_2$ dye, dye sensitized solar cells, electrochemical impedance spectroscopy
PACS No. 84.60.jt
* Corresponding authors, e-mail: rkurchania@gmail.com

1. Introduction

In recent decades [1-3], since the pioneering work of Michael Grätzel and coworkers [4], considerable research efforts have been devoted to dye sensitized solar cells (DSSCs). This can be attributed to their lower cost compared to inorganic photovoltaic technologies. The sensitizer is a key component of a DSSC, since its role is to efficiently harvest the light and inject the photogenerated electrons from the excited state into the conduction band of the metal oxide semiconductor. Many aspects of DSSCs have been investigated, including sensitizers, semiconducting metal oxide photoanodes, electrolytes and counter electrodes. These research efforts have resulted in the achievement of power conversion efficiencies (PCEs) up to 12.3 % for DSSCs [5]. Generally, DSSCs based on ruthenium complex based dyes show optimum efficiencies with the use of thick (> 15μm) TiO_2 photoanodes mainly because of their low molar extinction coefficient at maximum absorption wavelength peak due to metal to ligand charge transfer molecular excitation. On the other hand, metal free dyes compared to ruthenium complex based dyes, have larger molar extinction coefficients and allow fabrication of DSSCs with thinner TiO_2 photoanodes that minimize charge transport losses. The highest efficiency of metal free sensitizers based DSSCs have reached 10 % [6-9]. However, the sharp and narrow absorption band of the metal free dyes weakens the light harvesting capabilities over the whole visible spectrum. Enhancement of light harvesting efficiency may be achieved through incorporation of dyes that have broad absorption bands in the near infrared of the solar spectrum. However, the disadvantage of the single dye with wider absorption spectra is its difficulty to inject the photogenerated electron from sensitizer into the photoanode, if its LUMO level approaches the conduction band of TiO_2 [10-16]. Therefore, cosensitization of two dyes having complementary absorption is an effective approach to increase the photoanode light absorption behavior. Several research groups [17-23] have investigated DSSCs based on the cosensitization of two or more dyes

and found that the PCE of these devices had been improved significantly with respect to the DSSCs sensitized with individual dyes. Han *et al.* [21] has reported a very high PCE (11.4%) for DSSCs based on a cosensitized system of metal-free dye and black dye. A record high PCE of 12.3% is reported with two metal containing porphyrin dyes as co-sensitizers with the use of a Co (II/III) based redox electrolyte [5]. Recently 13 % PCE has been reported for DSSCs based on porphyrin dyes [24]. Several research groups [25-27] have used the cosensitization of two dyes using the molecular cocktail method but the success is limited due to the solubility of different dyes in a common solvent. Apart from this approach, step wise selective dye adsorption is a much simpler and inexpensive method for cosensitization of multiple sensitizers on a single TiO_2 electrode [28-32].

In this communication, we report a DSSC system using a well known Ru based dye i.e. N719 and metal free dye carbazole based D-(π-A)$_2$ i.e. 3,3'-(5,5'-(9-hexyl-9H-carbazole-3,6-diyl)-bis-(thiophene-5,2-diyl))-bis(2-cyanoacrylic acid) denoted as **D.** These are employed as primary and secondary sensitizers, respectively for cosensitization via a step wise adsorption approach to increase the PCE of the DSSC. The N719/**D** cosensitized DSSC shows a PCE of about 7.24 % which is higher than that of DSSCs based on either N719 (5.78 %) or **D** (3.95 %) sensitizers. The improved PCE of the cosensitized DSSC is attributed to the combined enhancement of both short circuit photocurrent (J_{sc}) and open circuit voltage (V_{oc}). These are non-optimized DSSC that do not contain $TiCl_4$ treatments or scattering layers.

2. Experimental details

Fluorine doped tin oxide (FTO) glass substrates were cleaned by sonication in decon 90, distilled water, isopropanol and finally with ethanol. The working electrodes for the DSSC were prepared by firstly forming a blocking layer from 0.2M di-isopropoxy titanium bis (acetylacetone) in isopropanol by spray pyrolysis. This was then followed by the deposition of a nano-crystalline layer of TiO_2 using the doctor blade technique using Dyesol

TiO_2 paste (DSL 18NR-T) on a pre-cleaned FTO coated glass substrate. The surface area of Dyesol TiO_2 paste (DSL-18NR, Dyesol) is 72.9 m^2/g. The TiO_2 coated FTO electrodes were heated at 500ºC for 30 min. The TiO_2 electrodes were then dipped in 0.02 M aqueous $TiCl_4$ for 20 minutes, rinsed with water and ethanol and annealed at 500ºC for 20 min. The thickness of the TiO_2 electrode was measured using a thin film thickness measurement system (Nano calc XR Ocean Optics Germany) and was found to be in the range 10-12 μm. The dye solutions were prepared using 5×10^{-4}M dye **D** in THF and 3×10^{-4}M N719 in acetonitrile/tert-butanol (1:1 v/v). For the cosensitization, the prepared TiO_2 photoanode was first dipped into the solution of N719 for 4 hrs before rinsing with ethanol and then dipping into the solution of **D** for a further 4 hrs. The counter electrode was prepared by spin coating of H_2PtCl_4 solution (2 mg of Pt in 1ml of isopropanol) onto the pre-cleaned FTO coated glass substrate and then heating at 450°C for 15 min in air. The sensitized working electrode was assembled with a Pt coated FTO electrode into a sandwich type cell and sealed with the hot-melt polymer Surlyn. To complete the DSSC fabrication, the electrolyte solution containing LiI (0.05M), I_2 (0.03 M), 1 methyl-3-n-propylimidazolium iodide (0.6M) and 0.5M tert-butylpyridine in a mixture of acetonitrile and valeronitrile (85:15 volume ratio) was introduced into the space between the two electrodes through a drilled hole in the Pt coated FTO by vacuum backfilling. DSSCs sensitized with N719 and **D** was also prepared for comparison. Moreover, cosensitized DSSCs were also prepared by dipping the photoelectrode firstly into the **D** solution followed by the N719 solution to determine if the order of application had any influence on performance.

The current–voltage (*J-V*) characteristics of the DSSCs under illumination (AM1.5, 100mW/cm^2) were measured with a computer controlled Keithley source meter (2601 A) and illuminated using the solar simulator TS space system class AAA. The incident photon to

current efficiency (IPCE) spectra of the DSSCs was measured using a Bentham IPCE system (TMc 300 monochromator computer controlled).

Electrochemical data were recorded using an Autolab Potentiostat/Galvanostat PGSTAT30. The cyclic voltammogram curves were obtained from a three electrode cell in 0.1 M Bu_4NPF6 N, N-dimethylformamide solution at a scan rate of 100 $mV.s^{-1}$, using a platinum wire counter electrode and Ag/AgCl reference electrode. The system was calibrated with ferrocene. Electrochemical impedance spectra was recorded using a CH Electrochemical workstation (CH-604D), of the DSSCs were measured in darkness, applying the dc biasing equivalent to the open circuit voltage in the frequency range 0.1 to 100 KHz.

3. Results and discussion

A D-$(\pi$-A$)_2$ metal free dye i.e. 3,3'-(5,5'-(9-hexyl-9H-carbazole-3,6-diyl)bis(thiophene-5,2-diyl))bis(2-cyanoacrylic acid) denoted as **D** with carbazole as a donor, cyanoacrylic acid as acceptor as well as anchoring group and thiophene as π-linker has been used as a second sensitizer along with the N719 dye for cosensitization. The Synthesis and characterization of metal free dye **D** has already been reported in literature [33]. The optical absorption spectrum of the **D** in solution is shown in Fig. 1. The band located at the shorter wavelength region is attributed to the π-π^* electron transition of chromophore. The absorption band at 265- 360 nm can be ascribed to localized aromatic π-π^* transitions. However, the absorption band at around 375–435 nm can be attributed to an intramolecular charge transfer between the carbazole donor and cyanoacetic acceptor [34]. It can be seen from Fig. 1 that the absorption maxima (λ_{max}) for **D** is 418 nm and the corresponding molar extinction coefficient is about 4.28 $x10^4$ M^{-1} cm^{-1} which is a higher value than that of 2.1 $x10^4$ M^{-1} cm^{-1} at 540 nm for the N719 dye. The fluorescence emission spectra of **D** exhibited stronger luminescence maxima in the wavelength region 490-550 nm recorded upon the excitation of absorption maximum value (Fig. 1). The zero-zero excitation energy ($E_{0\text{-}0}$) has

been estimated from the intersection point of emission and the corresponding absorption spectra, which is found to be 2.38 eV.

The absorption spectra of **D** on TiO_2 film is also shown in Fig. 1. The maximum absorption peak of **D** on TiO_2 is at about 430 nm. Compared to the solution spectra, the absorption band of **D** is redshifted by about 12 nm and also shows some broadening. This redshift can be explained by the formation of J-aggregates of the dye on TiO_2.

The ground state oxidation potential (E_{ox}) corresponding to the highest occupied molecular orbital level of **D** is about 1.04 V vs SCE (Saturated Calomel Electrode). This value is more positive than the redox potential of the I_3^- / I^- (0.4 V vs SCE [35-37]. This indicates that the oxidized dye formed after electron injection into conduction band of TiO_2 should be able to accept electrons from the I^- ions in the electrolyte [38]. The excited state oxidation potential *Eox** that corresponds to the lowest unoccupied molecular orbital (LUMO) energy level of sensitizer also plays an important role in the injection mechanism into the TiO_2 conduction band. The excited state oxidation potential is estimated using, $E_{ox}^* = E_{ox} - E_{0\text{-}0}$. The LUMO level of **D** is -1.34 V vs SCE which is more negative than the conduction band edge of the TiO_2 (-0.5 V vs SCE) [39, 40]. Since the difference in the LUMO of dye and conduction band edge of TiO_2 should be greater than 0.2 V this suggests that the electron injection process [41] is energetically favorable.

To obtain further insight into the electron distribution of the **D** dye, density functional theory (DFT) calculations have been performed at a B3LYP/6-31G* level using the Gaussian 09 program package [42]. The initial geometry optimizations have been performed using the Turbomole package [43]. The excitation transitions of the **D** have been calculated using time-dependent density functional theory (TD-DFT) calculations. We have calculated the optical gap both in gas phase as well as in the presence of solvents. The frontier molecular orbitals are shown in Fig. 2. The calculated parameter i.e. HOMO and LUMO energies, HOMO–

LUMO gap, optical gap with corresponding oscillator strength, and dipole moment (D) are compiled in Table 1. Solvent effects are taken into account for Tetrahydrofuran (THF). From Fig. 2, it can be seen that the carbazole contribution to the HOMO is 59 % and the remaining contribution is from thiophene π-spacer, while alkenes contributes less than 0.5 %. The situation is reversed for the LUMO in which we compute 88% contributions from the thiophene units along with anchoring carboxylic groups in **D**. The optical gaps computed using the B3LYP functional are in reasonable agreement with our experimental values, with a difference of only 0.37 eV.

Electronic binding of the anchoring group at the surface of TiO_2 has been investigated using FTIR spectroscopy of the pristine **D** powder and **D** adsorbed on the TiO_2 surface as shown in Fig. 3. For the pristine **D** powder, the C=O stretching band of the carboxyl group has been observed at 1724 cm^{-1} and characteristics stretching bands of C=N and C=C have been observed at 1585 cm^{-1} and 1384 cm^{-1}, respectively. When **D** is adsorbed onto the TiO_2 surface, the C=O stretching band at 1724 cm^{-1} disappears and the band corresponding to C=N is broadened. This indicates the formation of a strong bridging linkage between the carboxyl group of **D** and the Bronsted acid site on the TiO_2 surface [44].

The most commonly Ruthenium complex dye, N719, has been chosen as the primary sensitizer due to its wide absorption over visible region with absorption peaks at 540 nm (molar extinction coefficient 2.0 $x10^4$ $M^{-1}cm^{-1}$) and 400 nm (molar extinction coefficient 2.5 $x10^4$ $M^{-1}cm^{-1}$). The absorption peaks around 540 nm and 400 nm correspond to the metal to ligand charge transfer (MLCT) transition and MLCT along with a contribution from the π-π* transition.

The current–voltage characteristics of the DSSCs sensitized with N719 dye, **D** dye and N719/**D** and **D**/N719 are shown in Fig. 4 and the photovoltaic parameters are summarized in Table 2. The DSSC sensitized with only N719 yielded J_{sc} of 13.14 $mAcm^{-2}$,

V_{oc} of 0.62 V, FF of 0.71 and an overall PCE of 5.78 %. The DSSC based on only **D** sensitizer yielded J_{sc} of 9.34 mAcm^{-2}, V_{oc} of 0.58 V, FF of 0.73 and PCE of 3.95 %. However, the cosensitized (N719/**D**) DSSC shows a significant improvement in the device performance (J_{sc} = 14.63 mAcm^{-2}, V_{oc} = 0.66 V, FF = 0.75 and PCE = 7.24 %) over the individual sensitized N719 and **D** with the improvement in both J_{sc} and V_{oc}. On the other hand the cosensitized (**D**/N719) DSSC shows inferior performance (J_{sc} = 10.45 mAcm^{-2}, V_{oc} = 0.62, FF = 0.64 and PCE = 4.15 %) compared to the DSSC sensitized with N719. The PCE of DSSC cosensitized with N719/**D** shows higher J_{sc} when compared to the DSSCs sensitized with individual dyes.

The increase in the J_{sc} in DSSCs is related to the light harvesting efficiency of the photoanode used in the device, electron injection efficiency from the excited state of the sensitizer and charge collection efficiency. The light harvesting efficiency of the DSSC is directly related to the absorption profile of the dye adsorbed photoanode. To obtain information about the light harvesting capabilities of the different dye sensitized photoanodes, UV-Visible spectra of the photoanode adsorbed with **D**, N719 and N719/**D** has been carried out (as shown in Fig. 1 for **D** and Fig. 5 for N719 and N719/**D**). These figures indicate that the **D** possesses higher absorption intensity in the 400-450 nm region compared to N719. Therefore, upon co-sensitizing N719 with **D**, the absorption spectra of the N719/**D** adsorbed on to TiO_2 film demonstrates the panchromatic feature to provide an increased light harvesting efficiency. Since the LUMO level of both **D** (-1.34 vs SCE) and N719 (-0.94 V vs SCE) lies above the conduction band edge of TiO_2 (-0.5 V vs SCE), the electron injection from the LUMO level both dyes into the conduction band is energetically favorable. Moreover, the HOMO level of both dyes is more positive than the redox potential of I_3^- / I^- in the electrolyte and therefore supplies a thermodynamic driving force for dye regeneration [45-47]. The incident photon to current efficiency (IPCE) spectra of the DSSCs sensitized

with **D**, N719 and N719/**D** is shown in Fig. 6. It can be seen from Fig. 6 that the IPCE values at each wavelength are higher for the cosensitized DSSC than the individual dye sensitized DSSCs. Therefore, the cosensitization enhances the photoanode light harvesting capability and carrier generation across the whole visible region from 350 nm to 750 nm. The DSSC sensitized with N719 dye has only a broad IPCE spectrum extending from 350 nm to 750 nm and displayed the highest IPCE of about 47-63 % in the wavelength region 450 – 700 nm. The IPCE value decreases up to 32 % in the wavelength region 380 – 440 nm, which is attributed to the competitive light absorption between I_3^- and N719, since the molar extinction coefficient of I_3^- in this wavelength region is higher than that for the N719 dye [21]. However, the dip in the IPCE spectra is recovered for N719/**D** cosensitized DSSC probably because the molar extinction coefficient for the **D** dye in this region is higher than that for both I_3^- and N719 and the loss of light absorption by the I_3^- was suppressed by the **D** dye.

Dye loading of the photoanode is another important parameter for the PCE of DSSCs. The amount of dye loading on to the 12 μm thick sensitized TiO_2 photoanode is measured as described in the literature [32]. The amount of the dye loading for individual N719 and **D** coated photoanodes is approximately 0.45×10^{-7} mol.cm^{-2} and 0.98×10^{-7} mol.cm^{-2} respectively. However, the amount of N719 and **D** adsorbed in the cosensitized system is lower with values of 0.42×10^{-7} mol.cm^{-2} and 0.64×10^{-7} mol.cm^{-2}, respectively. In spite of this the total amount the co-sensitized dye molecules (N719/**D**) is increased by up to 1.6×10^{-7} mol.cm^{-2}. These results indicate that total coverage of TiO_2 surface has been improved by incorporating the small sized **D** molecules into gaps within the N719 dye adsorbed TiO_2 film. However, the total amount of dye adsorbed for the **D**/N719 system has been reduced, which may be due to the large molecular size of N719 when compared to **D**. When the TiO_2 photoanode is initially dipped into **D** before N719, the **D** completely adsorbed onto the TiO_2 surface. This

effectively hindered the subsequent absorption of the larger molecular sized N719 dye severely limiting its adsorption. The reduced dye loading for **D**/N719 suppresses the light harvesting efficiency and results in the lower PCE observed.

The J_{sc} is strongly influenced by the light harvesting efficiency, charge separation (such as injection dye regeneration and recombination) and charge collection. It has been reported that the cosensitization of dyes with co-adsorbents leads to breakup of dye aggregates, resulting in high PCE (mainly enhancement in J_{sc} and V_{oc}) [48-50].

Electrochemical impedance spectroscopy (EIS) provides information about the electron transport and recombination at the photoanode/dye/electrolyte interface in DSSCs [51-58]. EIS measurements are conducted to obtain information about interfacial charge transfer processes and the enhancement in PCE of the N719/**D** cosensitized DSSC. Impedance is measured over the frequency range 10^5 Hz to 0.1 Hz at room temperature in darkness with an applied voltage equivalent to the open circuit voltage of the DSSCs. Nyquist and Bode phase plots for the DSSCs sensitized with **D**, N719 and N719/**D** are shown in Fig. 7(a) and 7(b), respectively. The three semicircles from left to right in the Nyquist plots of the EIS represent the impedances of charge transfer at the Pt counter electrode (high frequency range), the charge transfer and recombination competition at the TiO_2/dye/electrolyte interface (middle frequency range), and electrolyte diffusion (low frequency range), respectively. To elucidate the interfacial charge transfer process, we have focused our attention on the large centrally located semicircle. This semi-circle gives information on recombination resistance (R_{ct}) and electron life time (τ_n). The electron life time is estimated from the peak frequency (f_{max}) in the Bode phase plots, as shown in Fig. 7(b) using $\tau_n = 1/2\pi f_{max}$. The charge collection efficiency is estimated from $\eta_{cc} = (1 + R_t / R_{ct})^{-1}$, where R_t is the electron transport resistance. The electron transport resistance (R_t) is manifested as a linear feature in the high frequency region of the central semicircle which indicates that the

electron transport features a transmission line behavior, which has been observed for DSSCs using TiO_2 photoanodes [52, 57]. An equivalent circuit based on the transmission line model [52-57] is applied yielding the EIS parameters, R_{ct}, R_t, C_μ, τ_n and η_{cc}, which are summarized in Table 3. The recombination resistance of the DSSC based on the N719/**D** is higher than that for the DSSCs sensitized with individual dyes, N719 or **D**. The cosensitization may induce the changes in the adsorption state of the dye and electronic states of the dye sensitized TiO_2, therefore influencing the electron injection efficiency [59, 60]. Therefore, the improved J_{sc} for the DSSC cosensitized with N719/**D** compared to DSSC with either N719 or **D** may be ascribed to the breakup of dye aggregates from the competitive coadsorption between N719 and **D**.

Improvement in the V_{oc} is generally related with the negative shift in the conduction band edge of TiO_2 or suppression of charge recombination. V_{oc} of DSSCs can be expressed as the voltage difference between the redox potential of the electrolyte (E_{redox}/q) and quasi Fermi potential of the TiO_2 as shown below [61].

$$V_{oc} = \frac{E_{cb}}{q} + \frac{kT}{q}\ln\left(\frac{n}{N_{cb}}\right) - \frac{E_{redox}}{q}$$

E_{cb} is the conduction band edge of TiO_2, N_{cb} is the density of states in TiO_2, n is the number of electrons in TiO_2 and q is the electronic charge. Since, we have used the same electrolyte in all DSSCs, E_{redox} is constant and the V_{oc} is only determined by the position of the TiO_2 E_{cb} and n. The dyes used as sensitizers can vary these two parameters. The conduction band (CB) of the TiO_2 can be affected by the surface charge induced by the interaction between the dye molecules and ions with TiO_2 at the interface. Any change in the surface charge will shift the E_{cb} of the TiO_2. The number of the electrons in the TiO_2 is related with the balance between the electron injection and recombination processes at the TiO_2/dye/electrolyte interfaces. The DSSC based on cosensitized N719/**D** has a longer

electron life time compared to the DSSC sensitized with either N719 or **D**. This suggests that the electron recombination with oxidized species of electrolyte has been reduced in the case of cosensitized DSSCs. Moreover, the total dye loading of DSSCs based on N719/**D** is higher than that for DSSCs sensitized with individual dyes, indicating better dye converge and a more compact layer. This compact layer prevents the penetration of electrolyte towards the TiO_2 surface. This reduces the recombination due to the back electron transfer between TiO_2, and I_3^- ions increasing the V_{oc} compared to those DSSC sensitized with individual dyes. Moreover, the recombination resistance (R_{ct}) is higher for N719/**D** system than the individual dyes, also support the reduction in dark current that results an improvement in V_{oc} for N719/**D** co-sensitized DSSC.

4. Conclusions

The optical and electrochemical properties of a metal free dye based on carbazole donor with double acceptor anchoring units, denoted as **D** and used as a co-sensitizer for DSSCs along with N719 dye has been investigated. In addition DFT simulations of the HOMO and LUMO frontier orbitals have been conducted.

It has been demonstrated that in a sequential stepwise co-sensitization process the co-sensitizers are selectively distributed on the TiO_2 surface due to differences in the molecular size of the sensitizers. The stepwise cosensitization starting with N719 i.e. N719/**D** was more effective than with **D**, i.e. **D**/N719. The overall PCE of the co-sensitized DSSCs was about 7.24 % compared to 3.95 % and 5.78 % for those sensitized with individual **D** and N719 dyes, respectively. The J_{sc} is improved because of the complementary absorption spectra, enhanced dye loading and favorable energy alignments of both **D** and N719 dyes. Improvements in V_{oc} are attributed to better surface coverage of the TiO_2 film forming a compact layer which helps to reduce the recombination due to the electron back reaction

between the injected electron in TiO_2 and I_3^- ions. The increase in both J_{sc} and V_{oc} lead to an enhancement in the overall PCE of the DSSC with step wise cosensitization.

Acknowledgements

Manjeet Singh is grateful to Maulana Azad National Institute of Technology (MANIT), Bhopal, India for Institute Fellowship for supporting his doctoral studies. Authors are thankful to UK India Education and Research Initiative (UKIERI-II) project coordinated by the British Council, New Delhi, India for financial support through a Thematic Partnership. Authors are also thankful to M. Chandrasekharam, Inorganic and Physical Chemistry Division, CSIR-Indian Institute of Chemical Technology, Hyderabad, India for providing the metal free dye **D**.

References

[1] M Gratzel *Acc. Chem. Res*. **42** 1788 (2009)
[2] A Hagfeldt, G Boschloo, L Sun, L Kloo and H Pettersson *Chem. Rev*. **110** 6595 (2010)
[3] M V Marınez-Dıaz, G de la Torre and T Torres *Chem. Commun*. **46** 7090 (2010)
[4] B O'Regan and M. Gratzel *Nature* **353** 737 (1991)
[5] A Yella *et al. Science* **334** 629 (2011)
[6] W Zeng *et al*. *Chem. Mater*. **22** 1915 (2010)
[7] A Mishra, M K R Fischer and P Bauerle Angew. *Chem. Int. Ed*. **48** 2474 (2009)
[8] A Hagfeldt, G Boschloo, L Sun, L Kloo and H Pettersson *Chem. Rev*. **110** 6595 (2010)
[9] Y S Yen, H H Chou, Y C Chen, C Y Hsu and J T Lin *J. Mater. Chem.* **22** 8734 (2012)
[10] A Abbotto *et al*. *Dalton Trans.* **40** 234 (2011)
[11] S Paek *et al*. *Chem. Commun*. **47** 2874 (2011)
[12] Y Liu *et al*. *Chem. Commun*. **47** 4010 (2011)
[13] T Maeda, Y Hamamura, K Miyanaga, N Shima, S Yagi and H Nakazumi *Org. Lett*. **13** 5994 (2011)
[14] S Gomez Esteban, P de la Cruz, A Aljarilla, L M Arellano and F Langa *Org. Lett*. **13** 5362 (2011)
[15] A Braga, S Gimenez, I Concina, A Vomiero and I N Mora-Sero J. Phys. *Chem. Lett*. **2** 454 (2011)
[16] C Jiao, N Zu, K-W Huang, P Wang and J Wu *Org. Lett*. **13** 3652 (2011)
[17] K M Lee *et al*. *J. Power Sources* **196** 2416 (2011)
[18] J Waman, F Buschest, Y Pellegtin, E Blart and F Odobel *Org. Lett*. **13** 3944 (2011)
[19] R Y Ogura, S Nakane, M Morooka, M Orihashi, Y Suzuki and K Noda *Appl. Phys. Lett*. **94** 073308 (2009)
[20] C M Lan *et al. Energy Environ. Sci*. **5** 6460 (2012)
[21] L Han *et al. Energy Environ. Sci*. **5** 6057 (2012)
[22] H Ozawa, R Shimizu and H Arakawa *RSC Adv*. **2** 3198 (2012)
[23] J H Yum, E Baranoff, S Wenger, M K Nazeeruddin and M Gratzel *Energy Environ. Sci.* **4** 842 (2011)
[24] S Mathew *et al. Nature Chemistry* **6** 242 (2014)
[25] J J Cid *et al. Angew. Chem. Int. Ed.* **46** 8358 (2007)
[26] B-W Park *et al. Appl. Phys. Express* **4** 012301 (2011)
[27] T Ono, T Yamaguchi and H Arakawa *Sol. Energy Mater. Sol. Cells* **93** 831 (2009)
[28] D Kuang *et al*. *Langmuir* **23** 10906 (2007)
[29] S-Q Fan *et al*. *J. Phys. Chem. C* **115** 7747 (2011)
[30] C-M Lan *et al. Energy Environ. Sci*. **5** 6460 (2012)
[31] K-M Lee *et al. J. Power Sources* **196** 2416 (2011)
[32] L H Nguyen *et al. Phys. Chem. Chem. Phys*. **14** 16182 (2012)
[33] K S V Gupta *et al. Organic Electronics* **15** 266 (2014)
[34] S Roquet *et al. J. Am. Chem. Soc*. **28** 3459 (2006)
[35] Q Wang, J E Moser and M Gratzel *J. Phys. Chem. B* **109** 14945 (2005)
[36] A Burke, S Ito, H Snaith, U Bach, K Kwiatkowski and M Gratzel *Nano Lett*. **8** 977 (2008)
[37] Z J Ning *et al*. *J. Phys. Chem. C* **113** 10307 (2009)
[38] C Klein, M K Nazeeruddin, D D Censo, P Liska and M Gratzel *Inorg. Chem*. **43** 4216 (2004)
[39] S Hwang *et al. Chem. Commun*. 4887 (2007)
[40] W Wu *et al. J. Mater. Chem*. **20** 1772 (2010)
[41] S Ito *et al*. *Adv. Mater*. **18** 1202 (2006)

[42] M J Frisch *et al. Gaussian 03 version C01* (Wallingford CT: Gaussian, Inc) (2004)
[43] TURBOMOLE *(version 5.6)* Universitat Karlsruhe (2000)
[44] Z S Wang *et al. J. Phys. Chem. B* **109** 3907 (2005)
[45] M Wang *et al. Nano Today* **5** 169 (2010)
[46] Y Cao *et al. J. Phys. Chem. C* **113** 6290 (2009)
[47] J Y Kim, Y H Kim and Y S Kim *Curr. Appl. Phys.* **11** S117 (2011)
[48] B J Song *et al. Chem A–Eur. J.* **17** 11115 (2011)
[49] S H Kang *et al. J. Mater. Chem. A* **1** 3977 (2013)
[50] H M Song *et al. J. Mater. Chem.* **22** 3786 (2012)
[51] R Kern, R Sastrawan, J Ferber, R Stangl and J Luther *Electrochim. Acta* **47** 4213 (2002)
[52] J Bisquert *J. Phys. Chem. B* **106** 325 (2002)
[53] J Bisquert *Phys. Chem. Chem. Phys.* **5** 5360 (2003)
[54] F Fabregat-Santiago, J Bisquert, G Garcia-Belmonte, G Boschloo and A Hagfeldt *Sol. Energy Mater. Sol. Cells* **87** 117 (2005)
[55] Q Wang *et al. J. Phys. Chem. B* **110** 25210 (2006)
[56] F Fabregat-Santiago *et al. J. Am. Chem. Soc.* **131** 558 (2009)
[57] J Bisquert, F Fabregat-Santiago, I Mora-Sero, G Garcia-Belmonte and S J Gimenez *J. Phys. Chem. C* **113** 17278 (2009)
[58] J Nissfolk, K Fredin, A Hagfeldt and G Boschloo *J. Phys. Chem. B* **110** 17715 (2006)
[59] Z Zhang, S M Zakeeruddin, B O'Regan, R Humphry-Baker and M Gratzel *J. Phys. Chem. B* **109** 21818 (2005)
[60] N Kopidakis, N R Neale and A J Frank *J. Phys. Chem. B* **110** 12485 (2006)
[61] M A Green *Solar Cells: Operating Principles, Technology and System Applications* (Englewood Cliffs NJ: Prentice-Hall) (1982)

Table 1
Calculated HOMO and LUMO energies (eV), HOMO–LUMO gap (eV), optical gap (eV) with corresponding oscillator strength and dipole moment (D) of the dye **D** structures in gas phase and THF solvent

Phase	HOMO (eV)	LUMO (eV)	HL gap (eV)	Optical gap (eV)	Oscillator strength	Dipole moment (D)
Gas phase	-5.86	-2.95	2.92	2.80	0.08	9.49
THF phase	-5.77	-3.01	2.76	2.39	1.37	11.23

Table 2
Photovoltaic parameters of DSSCs based on **D**, N719, N719/**D** and **D**/N719

Dye system	J_{sc} (mAcm^{-2})	V_{oc} (V)	FF	PCE (%)	Overall dye loading (mol.cm^{-2})
D	9.34	0.58	0.73	3.95	0.45 x10^{-7}
N719	13.14	0.62	0.71	5.78	0.98 x10^{-7}
N719/**D**	14.63	0.66	0.75	7.24	1.6 x10^{-7}
D/N719	10.45	0.62	0.64	4.15	0.56x10^{-7}

Table 3
EIS parameters and charge collection efficiency of DSSCs. Calculated values are from EIS data in dark conditions measured at forward bias of -0.6 V

Dye system	R_t (Ohmcm^2)	R_{ct} (Ohmcm^2)	C_μ (mF)	τ_n (ms)	η_{cc}
D	15.7	32	6.8	22	0.67
N719	13.6	53	6.4	34	0.79
N719/**D**	11.8	78	6.78	53	0.87

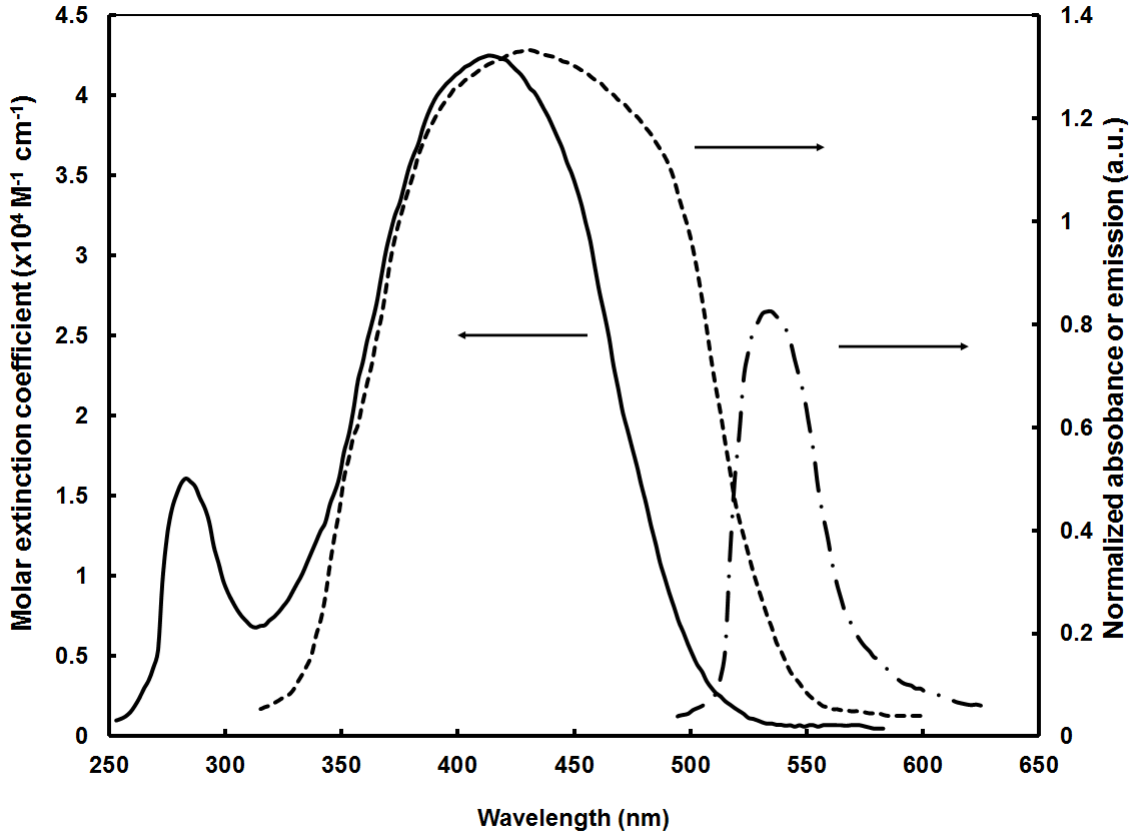

Figure 1

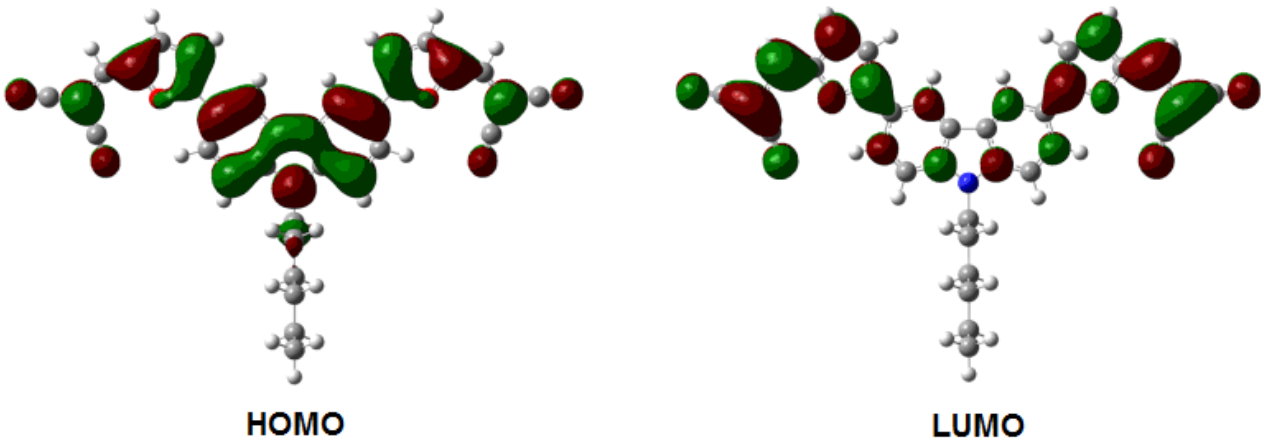

Figure 2

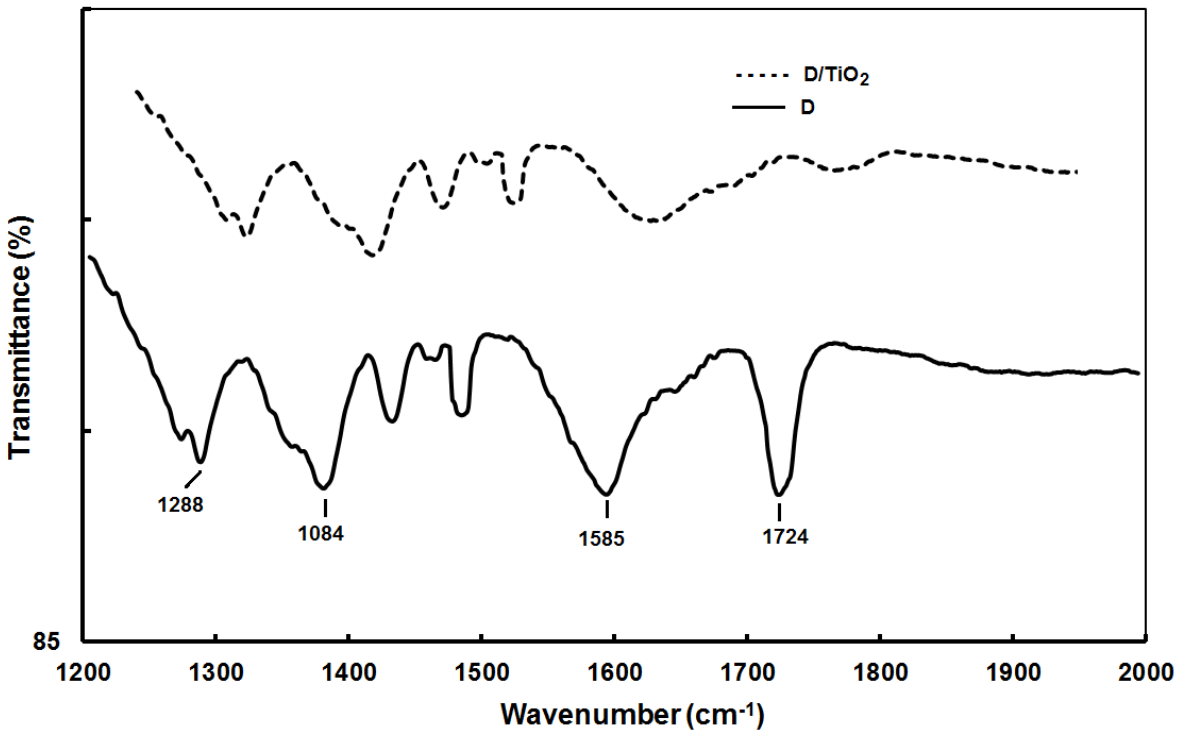

Figure 3

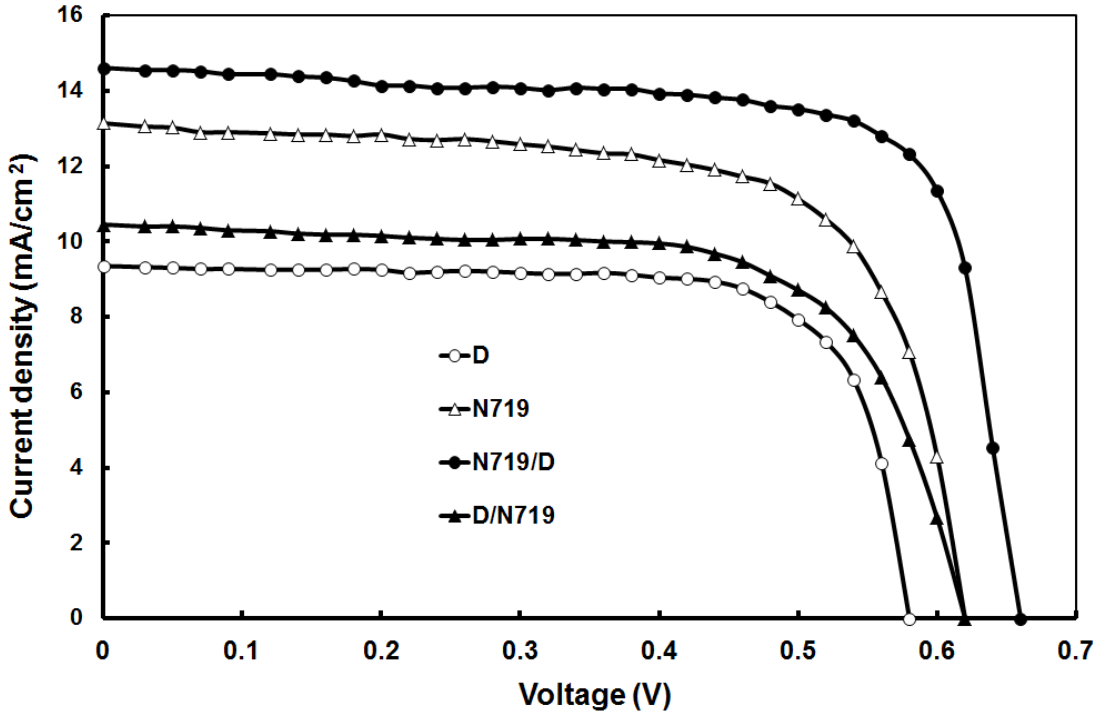

Figure 4

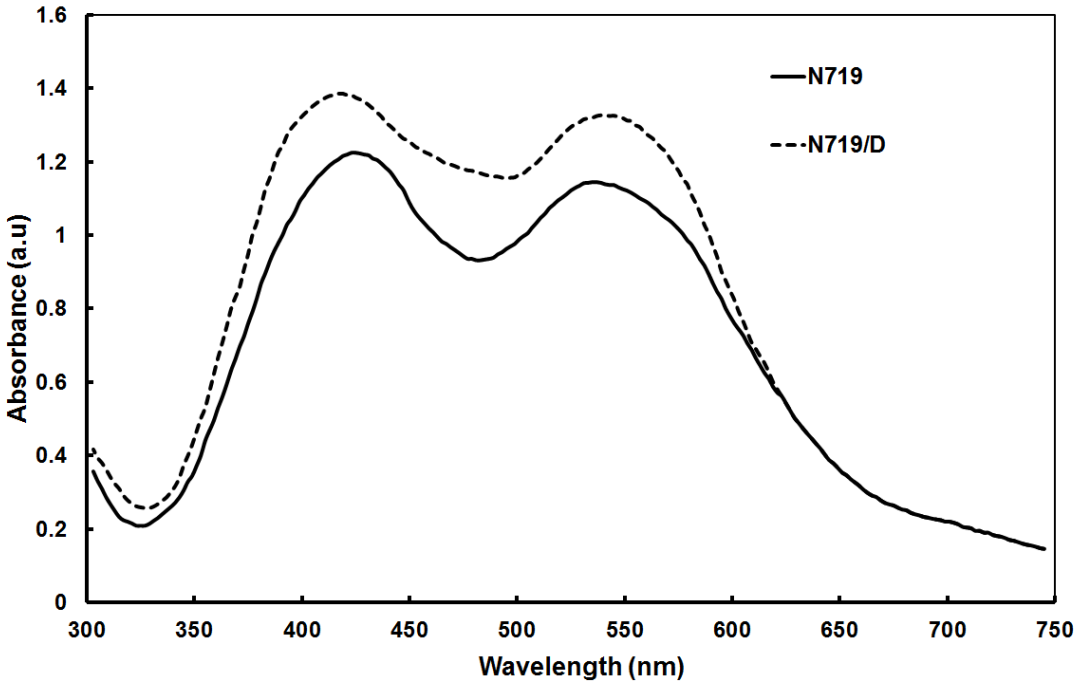

Figure 5

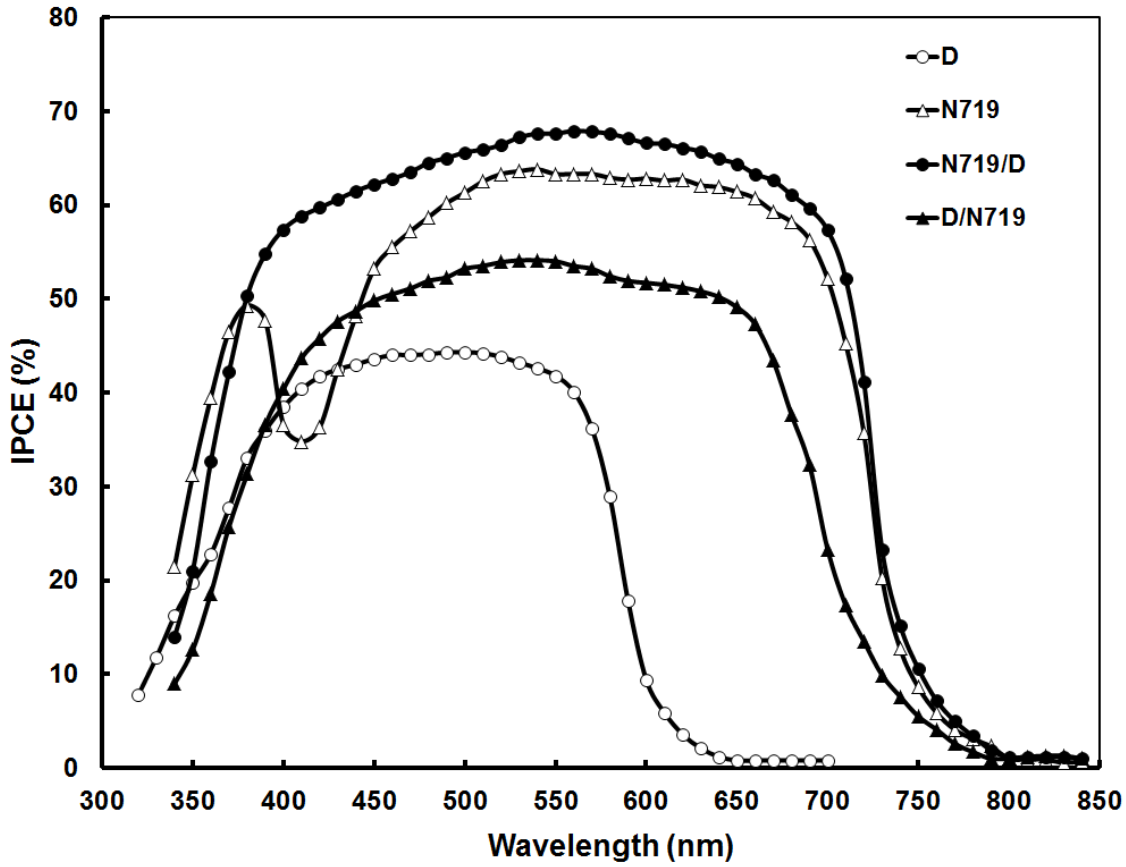

Figure 6

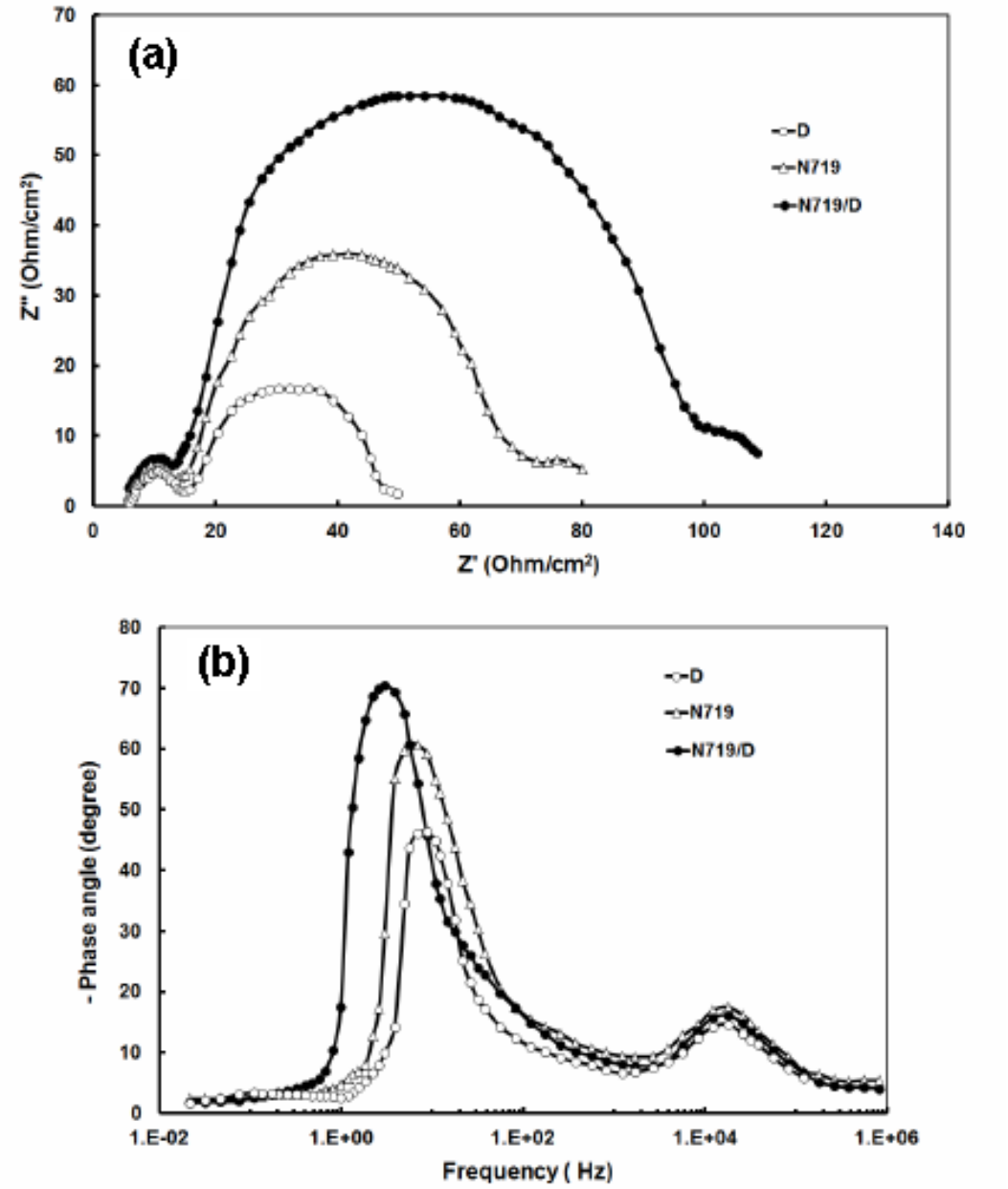
(a)
D
N719
N719/D
Z'' (Ohm/cm²)
Z' (Ohm/cm²)
0
10
20
30
40
50
60
70
0
20
40
60
80
100
120
140
(b)
D
N719
N719/D
- Phase angle (degree)
Frequency (Hz)
0
10
20
30
40
50
60
70
80
1.E-02
1.E+00
1.E+02
1.E+04
1.E+06

Figure 7

Figure captions

Figure 1 Absorption spectra **D** in solution, adsorbed on to TiO_2 film and emission spectra of **D**

Figure 2 Molecular frontier orbitals of dye **D**

Figure 3 FTIR spectra of **D** and **D** adsorbed on to TiO_2

Figure 4 Current–voltage (J-V) characteristics of cosensitized (N719/D and D/N719) DSSC and sensitized with D and N719, under illumination (100 mW/cm^2)

Figure 5 Optical absorption spectra of N719 and N719/**D** adsorbed onto the TiO_2 surface.

Figure 6 IPCE spectra of DSSCs sensitized with **D**, N719, N719/**D** and **D**/N719

Figure 7(a) Nyquist and (b) Bode phase plots from the EIS spectra for the DSSCs sensitized with **D**, N719 and N719/**D** in dark conditions